ELSEVIER

Ceramics International 25 (1999) 617–622

CERAMICS INTERNATIONAL

Fabrication of unglazed floor tiles containing Iranian copper slags

V.K. Marghussian [a,*], A. Maghsoodipoor [b]

[a] *Ceramics Division, Department of Materials, Iran University of Science and Technology, Narmak, Tehran 16844, Iran*
[b] *Materials and Energy Research Center, PO Box 14155, 4777 Tehran, Iran*

Received 30 March 1998; received in revised form 6 June 1998; accepted 1 September 1998

Abstract

Thermal behaviour of reverberatory furnace copper slag was investigated using simultaneous thermal analysis (STA), dilatometry and X-ray diffraction techniques. The results were used to study the effect of progressive addition of copper slag to a standard floor tile body formulation. It was observed that SO_2 emission at high temperatures resulted in bloating of the bodies, limiting the possibility of slag addition to a maximum of 40 wt%. The most promising body, containing 40 wt% copper slag, after firing at 1025°C for 1 h had a bend strength of 57 MN m^{-2}, water absorption of 2 wt%, hardness of 750 HV and a very good acid resistance.

Keywords: Unglazed floor tiles; Copper slag

1. Introduction

Slags, industrial by-products from metallurgical plants, have found many diverse applications, from production of hydraulic cements to ceramic building products and glass-ceramic materials. In the field of building ceramics, many investigations have been carried out on the use of slags, especially iron slags, as a raw material in the formulation of wall and floor tiles. Mizdut [1] reported on the production of wall tiles with no firing shrinkage containing up to 65 wt% iron slags. Myers et al. [2] have formulated wall tiles containing 25 wt% iron slag, exhibiting a firing shrinkage of $<1\%$. In Italy [3], 25–40 wt% iron slags have been added to a mixture of clays to produce wall tiles of good mechanical strength, and less than 1% firing shrinkage on 30 min firing cycles. Del Bufalo [4], Mascolo et al. [5], Sersale et al. [6] and Colella et al. [7] have also formulated various iron slag containing bodies in the field of building ceramics. In Iran [8] wall tile bodies containing 30 wt% blast furnace slag were formulated which after 5 min firing at 1060°C gave a bend strength of 24 MN m^{-2}, water absorption of 16 wt% and a firing shrinkage of 0.1%. Nel and Tauber [9] used up to 75 wt% south African iron slags in the formulation of floor tiles and bodies of 0.2 wt% water absorption and bend strength of 43.8 MN m^{-2} were obtained. Hinz et al. [10] processed a ''sinter slag'' material from a copper slag, which after dry pressing and firing at 1080–1130°C in a reducing atmosphere, exhibitied a very high strength and low porosity.

In the present investigation an Iranian copper slag was used for the first time in formulating unglazed floor tiles and the reaction sequences, phase compositions developed at each stage of firing and the physical properties of fired products were investigated.

2. Experimental procedure

2.1. Raw materials

Local raw materials, namely a reverberatory furnace copper slag from the Iranian National Copper Industries Co., a pyrophilitic clay (clay A) from Abadeh, a very plastic clay (clay B) from Latian, a feldespatic sand (sand C) and a quartzeous sand (sand D) were used. The chemical and mineralogical compositions of these materials are given in Tables 1 and 2, respectively. A base body composition was first formulated by using the clay and sand constituents and then the slag was added to it to make the experimental body compositions.

Tables 3 and 4 give the base body composition and the composition of experimental bodies on raw material

* Corresponding author. Fax: +98-745-4057.

0272-8842/99/$ - see front matter
PII: S0272-8842(98)00075-3

Table 1
Chemical composition of raw materials (wt%)

Oxide	Copper slag	Clay	Sand		
		A	B	C	D
SiO_2	40.97	49.8	64.0	74.6	97.5
Al_2O_3	3.78	27.6	15.8	9.8	1.0
Fe_2O_3[a]	44.78	9.2	1.8	1.5	0.2
TiO_2	0.58	–	–	0.2	–
CaO	5.24	1.7	5.6	3.2	0.5
MgO	1.16	0.6	2.0	0.3	–
Na_2O	0.3	1.4	0.9	3.3	–
K_2O	2.03	1.9	1.6	2.2	–
S	1.06	–	–	–	–
LOI	–	7.8	8.2	4.7	0.5

[a] The slag actually contained $FeO + Fe_2O_3$ which is represented as Fe_2O_3.

basis, whereas Table 5 represents the compositions of experimental bodies on oxide content basis.

2.2. Powder preparation and processing

A batch of base composition was first prepared by wet grinding raw materials in a ball mill for different times to obtain a residue of 5–7 wt% on a 63 μm (230 ASTM) mesh sieve. After drying the slurries, the experimental body mixtures were prepared by combining the base body batch with ground slag in different proportions according to Table 4. The mixtures were wet ground in a fast mill for 5 min and dried. The dried bath mixtures were then brought to a moisture content of 5 wt%, left to equilibrate for 24 h in a closed container and then were forced through a 0.84 mm (20 ASTM) mesh sieve for granulation purposes. The granulated powder were pressed in two steps using a laboratory hydraulic press, into 50×50×5 mm tiles, at initial and final pressures of 12 and 35 $NM\,m^{-2}$, respectively.

Table 2
Mineralogical composition of raw materials

Raw material	Major crystalline phases (in descending order)
Copper slag	$2FeO.SiO_2$, Fe_3O_4, $Ca(Fe,Mg)(Si_2O_6)$
Clay A	Pyrophilite, quartz, muscovite, feld spar, calcite, goethite
Clay B	Montmorilonite, quartz, kaolinite, mica
Sand C	Quartz, albite, illite/muscovite
Sand D	Quartz

Table 3
Base body composition on raw material basis (wt%)

Raw material	Clay A	Clay B	Sand C	Sand D
Wt%	50	15	15	20

Table 4
Composition of experimental bodies on raw material basis (wt%)

Body	% slag	% base body
A	0	100
B	20	80
C	40	60
D	60	40
E	80	20
F	100	0

2.3. Firing

The specimens after drying at 110°C in a laboratory dryer, were fired at 1000, 1025, 1050 and 1075°C in an electric furnace at a rate of 5 $K\,min^{-1}$.

To identify the phases developed at different stages of firing, the specimens were taken out of the furnace after a 1 h soak at each predetermined temperature. For the determination of linear shrinkage, water absorption and bend strength the specimens were furnace cooled after soaking at the peak temperature for 1 h.

2.4. Properties characterisation

The linear shrinkage, water absorption, bend strength and microhardness were determined for each specimen. For the linear shrinkage the length of each specimen was measured to 0.05 mm before and after firing.

Water absorption was determined according to the procedure described in ASTM C373 [11]. The bend strength was measured in four point bending with spans of 40 and 20 mm on an Instron universal testing machine using rectangular bars of 45×14×5 mm dimensions. On average six specimens were used for each strength measurement. The microhardness was measured by the Vickers diamond pyramid test, on polished specimens. Five indentations were made for each specimen with a time of 30 s at a load of 200 g.

The materials were also characterised by X-ray diffractometry (XRD), simultaneous thermal analysis

Table 5
Chemical composition of experimental bodies (wt%)

Oxide	Body					
	A	B	C	D	E	F
SiO_2	65.19	60.34	55.50	50.65	45.81	40.97
Al_2O_3	17.84	15.02	12.21	9.40	6.59	3.78
Fe_2O_3	5.13	13.06	21	28.92	36.85	44.78
TiO_2	0.03	0.14	0.25	0.36	0.47	0.58
CaO	2.27	2.86	3.45	4.05	4.64	5.24
MgO	0.65	0.75	0.85	0.95	1.05	1.16
K_2O	1.52	1.62	1.72	1.82	1.92	2.03
Na_2O	1.33	1.12	0.92	0.71	0.50	0.3
S	–	0.21	0.42	0.63	0.85	1.06
LOI	5.63	4.50	3.37	2.25	1.12	–

(STA) and dilatometric techniques. The heating rates were 25 and 5 K min^{-1} in STA and dilatometric tests, respectively.

3. Results and discussion

3.1. Fired properties

Fig. 1 shows that all specimens exhibited a permanent shrinkage after 1 h heating at 1000°C. Increasing the soaking temperature from 1000 to 1025°C resulted in more intense shrinkage, but a further temperature increase up to 1075°C first reduced the shrinkage and then caused a marked expansion in all slag containing specimens. The results of water absorption vs firing temperature shown in Fig. 2 indicates that by increasing the soaking temperature from 1000 to 1025°C the water absorption was decreased, due to the densification of specimens as a result of sintering. A further temperature increase from 1025 to 1075°C resulted in considerable water absorption increase. The bend strength vs firing temperature results shown in Fig. 3 indicates that by increasing the soaking temperature from 1000 to 1075°C the bend strength was first increased (1000–1025°C range) and then decreased, supporting the linear shrinkage and water absorption results. These results all suggest the possible occurrence of a bloating process in the slag containing specimens in the 1025–1075°C range.

3.2. STA (DTA/TG) results

Fig. 4 depicts the STA results performed on a copper slag specimen. The TG curve reveals the occurrence of a marked weight gain in the 374–989°C range, following by a weight loss from 989 to 1040°C and a nearly constant weight region of 1040–1200°C. The exothermic peaks at 516 and 767°C in DTA trace can be related to the magnetite→maghemite and maghemite→hematite transformations, respectively [12]. The endothermic dip at 1040°C probably can be associated with the slag melting.

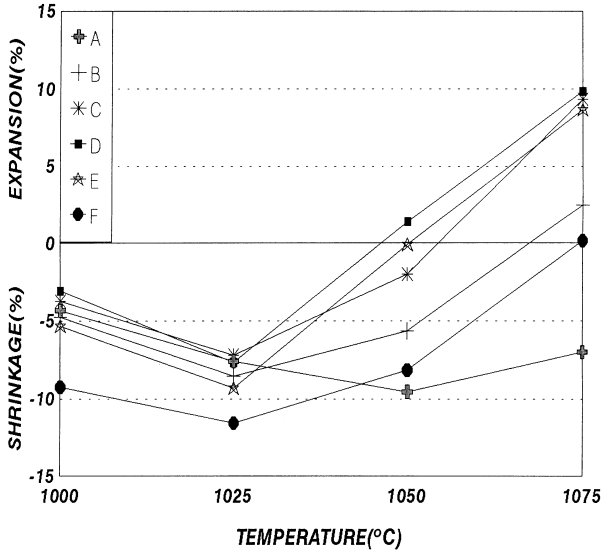

Fig. 1. Permanent linear change vs firing temperature for specimens containing differing amounts of copper slag.

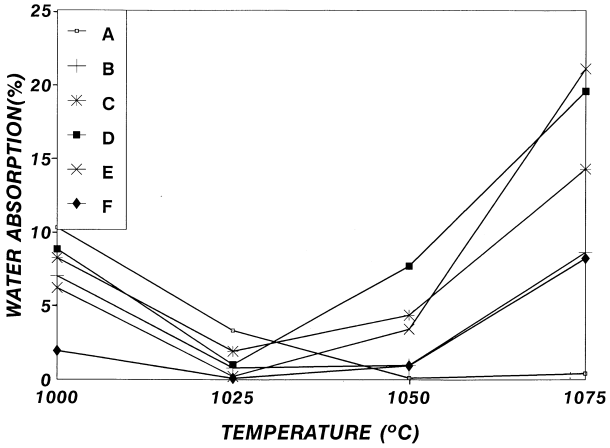

Fig. 2. Water absorption vs firing temperature for specimens containing differing amounts of copper slag.

3.3. X-ray diffractometry

Fig. 5 illustrates the slag XRD patterns at various stages of firing. The major crystalline phases present after firing at 400°C were fayalite ($2FeO.SiO_2$), magnetite

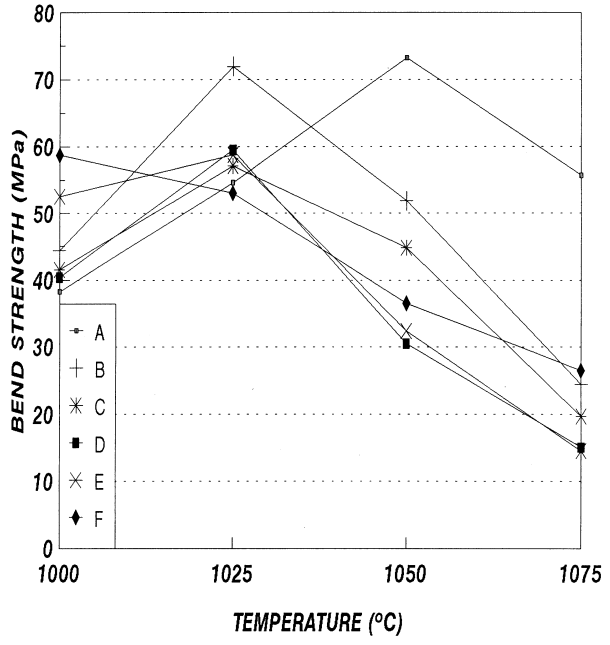

Fig. 3. Bend strength vs firing temperature for specimens containing differing amounts of copper slag.

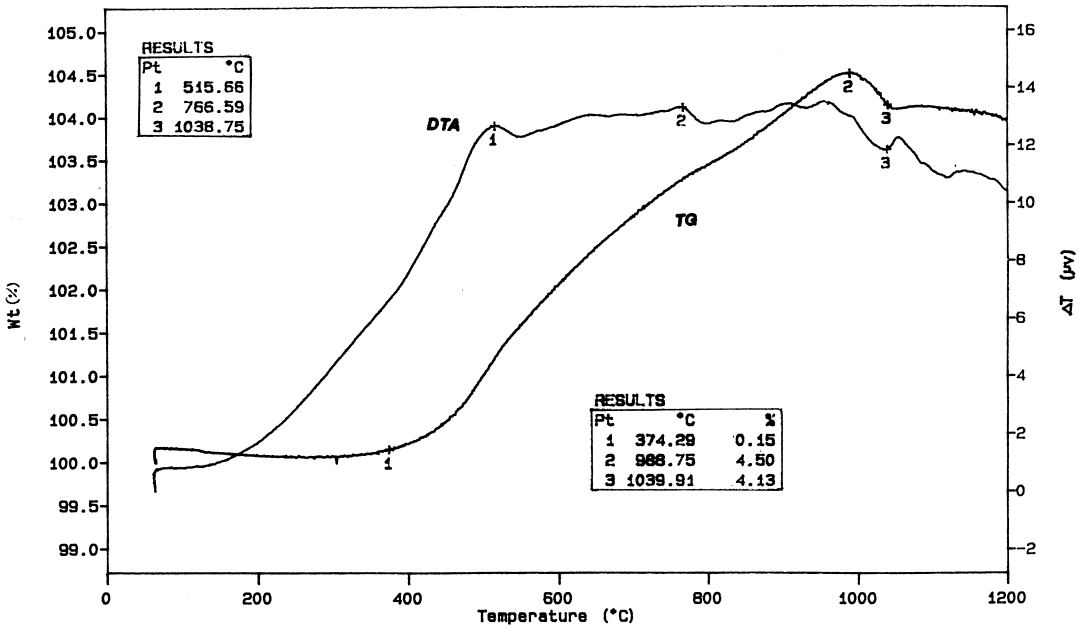

Fig. 4. STA (TG/DTA) traces of copper slag.

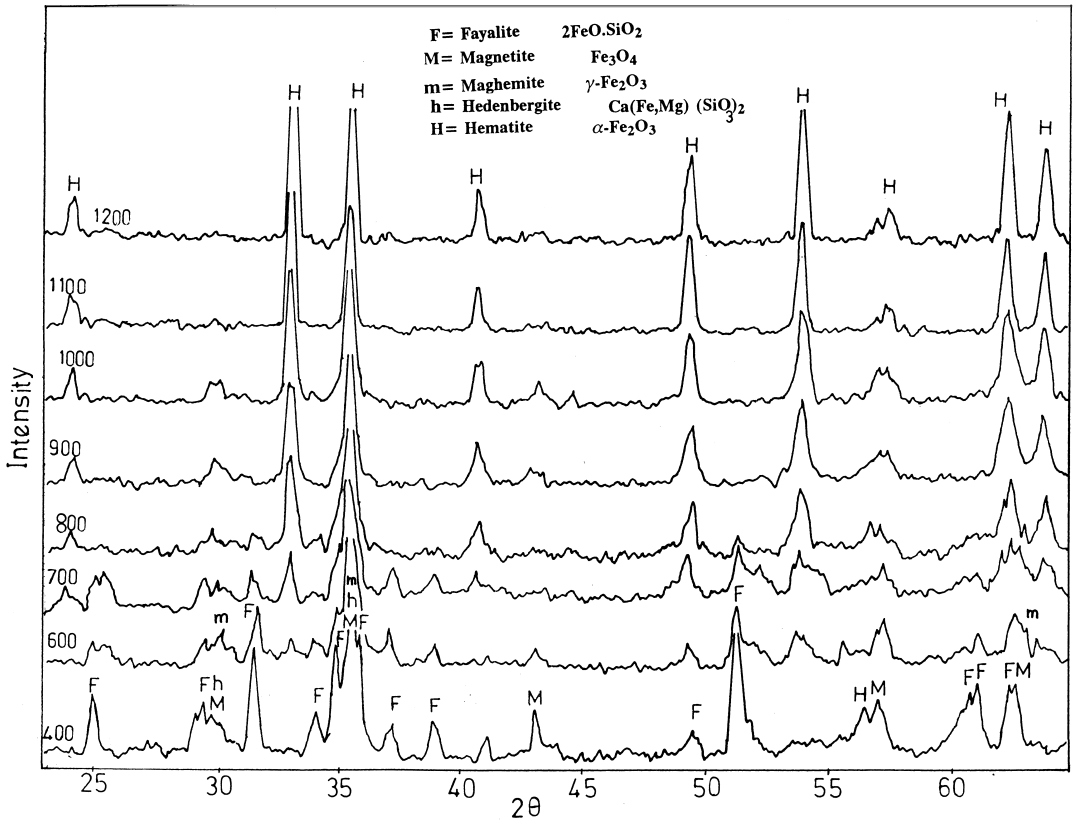

Fig. 5. XRD traces of copper slag at different firing temperatures.

(Fe_3O_4), hedenbergite $Ca(Fe,Mg)(SiO_3)_2$ and hematite (α-Fe_2O_3). By increasing the temperature to 600°C the magnetite peaks disappeared from the XRD pattern, whereas the maghemite (γ-Fe_2O_3) peaks appeared and the fayalite peak heights decreased. As the temperature rise continued maghemite and fayalite peaks disappeared in the 700–800 and 600–1000°C ranges, respectively.

3.4. The cause of bloating

From the STA and XRD results it can be concluded that the weight gain observed in the 374–989°C range (Fig. 4) is mainly due to the oxidation of fayalite according to the following reaction:

$$2FeO.SiO_2 + \frac{1}{2}O_2 \rightarrow \alpha - Fe_2O_3 \text{ (hematite)} + SiO_2 \quad (1)$$

The absence of any silica peaks in the X-ray diffraction patterns indicated the possible amorphous structure of the silica phase formed according to reaction (1) above. The weight loss observed >989°C (Fig. 4) can probably be associated with the oxidation of copper and iron sulphides present in minor amounts in the copper slag. To verify this deduction the furnace exhaust gases were analysed at different temperatures and the presence of SO_2 was confirmed in the temperature range of ~800–1200°C. Therefore it can be concluded that the weight loss due to the oxidation of sulphides was counterbalanced by the weight gain of fayalite oxidation up to 989°C, above which the weight loss process predominated. Above 1040°C the partial melting of slag probably prevented the gas escape and stopped the weight loss process.

To verify the cause of the endothermic dip observed at 1040°C in the DTA trace, a dilatometric test was performed on the slag. As shown in Fig. 6 the considerable shrinkage of the specimen in 975–1000°C range, confirms our previous assumption concerning the commencement of the melting process in this temperature range. The difference observed in the peak temperatures of the DTA and dilatometric traces probably resulted from the different heating rates employed in these tests. Considering the experimental evidence, the bloating of specimens can therefore be attributed to the SO_2 emission accompanied by partial melting of slag, preventing free gas escape. Obviously the slag viscosity which depends on the composition and temperature is the most significant factor in this connection. This fact explains the observed differences regarding the behaviour of various specimens in the dimensional change vs temperature experiments. For example, specimen D, containing 60 wt% slag, exhibited the largest thermal expansion (bloating) >1075°C (Fig. 1), whereas specimen F (pure slag) showed almost no dimensional change at this temperature. This can be attributed to the composition differences. Specimen D containing more silica and less iron oxide was more refractory and developed a melt of higher viscosity, which in comparison with the liquid phase of composition F, prevented the gas escape more severly and caused more extensive bloating.

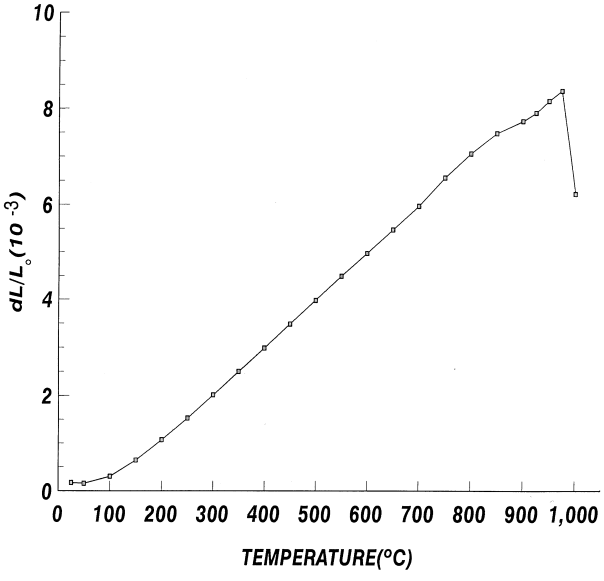

Fig. 6. Dilatometric trace for copper slag.

3.5. The most promising specimens

Fig. 7 shows the dimensional changes for different specimens in the 1000–1050°C range. It can be seen that specimens B and C showed the best tolerance towards temperature changes. These spesimens also exhibited acceptable values for bend strength and water absorption. Specimen C containing more slag, which after firing at 1025°C gave a bend strength of 57 NM m^{-2}, 2 wt% water absorption and a microhardness of 750 $VH_{(200)}$ can be used as a standard unglazed floor tile.

3.6. Acid resistance

The presence of relatively little alkali oxides and large amounts of Fe_2O_3 and Al_2O_3 in the composition of specimen C, indicated the possibility of a high resistance to acids for these specimens. Performance of an acid

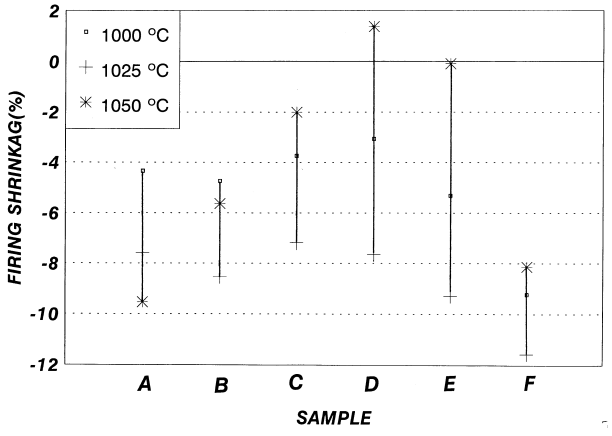

Fig. 7. Dimensional changes for various specimens fired in the 1000–1050°C range.

resistance test according to the procedure described in the ASTM C279 [13] revealed the excellent resistance of them against mineral acids (Type III for use where minimum absorption and maximum acid resistance are required), with higher water absorption values, but a very low weight loss (<2 wt%) as compared to the requirments of the ASTM standard.

4. Conclusions

1. Addition of 20–80 wt% copper slag to a standard floor tile composition increased the firing shrinkage and bend strength values and decreased the water absorption, up to a firing teperature of 1025°C, for all specimens.
2. The increase of firing temperature from 1025 to 1075°C reversed the firing behaviour of all slag containing specimens, resulting in lower bend strength and higher water absorption values owing to occurence of a bloating process.
3. Performance of STA (TG/DTA) and XRD tests on copper slag revealed the transformations of fayalite to hematite and amorphous silica, magnetite to maghemite and hematite and emission of SO_2 due to the oxidation of sulphides.
4. Emission of SO_2 was mainly responsible for the occurence of the bloating process.
5. An optimum slag content, which in the present investigation was 40 wt%, may be found which gives the best combination of properties.
6. The most promising specimens had a high resistance to mineral acids and may be used as acid resistant tiles.

References

[1] H. Mizdut, Nagoya Kogyo Gijutsu Shkensho HoKuKo (Rep. Govt. Res. Inst., Nagoya) 1 (1976) 40.
[2] V.D. Myers, W. Simpson, G. Weiss, Glastech. Ber. 50 (1977) 81.
[3] C. Fiori, A. Brusa, in: P. Vincenzini (Ed.), Ceramic Powders, Elsevier Scientific, New York, 1983, pp. 173–183.
[4] S. Del Bufalo, Ceramica Inform. 9 (1979) 459.
[5] G. Mascolo, E. Iannone, C. Colella, Ceramurgia 8 (1978) 257.
[6] R. Sersale, R. Aiello, C. Colella, G. Frigione, Silic. Ind. 12 (1976) 513.
[7] C. Colella, G. Mascolo, A. Nastro, R. Aiello, La Ceramica 2 (1981) 12.
[8] V.K. Marghussian, B. Eftekhari Yekta, Brit. Ceram. Trans. 93 (1994) 141.
[9] P.J. Nel, A. Tauber, J. South Afr. Inst. Min. Met. 70 (1970) 336.
[10] W. Hinz, W. Muller, F.G. Wishmann, Silikattechnik 17 (1966) 6.
[11] Standard test method for water absorption, bulk density, apparent porosity and apparent specific gravity of fired whiteware products, ASTM Standard C373-72, ASTM, Philadelphia, PA, 1972.
[12] Mackenzie, R.C., Differential Thermal Analysis, vol. 1, Academic Press, London, 1970, pp. 272–275.
[13] Standard specification for chemical-resistant masonary units, ASTM Standard, C279-88, ASTM, Philadelphia, PA, 1988.